Article citation info:
Kamiński A, Krakowian K, Skrętowicz M, Kupski M. Efficiency optimization of a vehicle combustion engine by the adjustment of the spark advance angle. Combustion Engines. 2024;196(1):10-14. https://doi.org/10.19206/CE-175071

Adam KAMIŃSKI
Konrad KRAKOWIAN
Maria SKRĘTOWICZ
Mateusz KUPSKI

Combustion Engines
Polish Scientific Society of Combustion Engines

Efficiency optimization of a vehicle combustion engine by the adjustment of the spark advance angle

ARTICLE INFO

Received: 31 May 2023
Revised: 27 October 2023
Accepted: 10 November 2023
Available online: 16 December 2023

Changing the ignition advance angle has a significant impact on the performance of a combustion engine. Optimization of ignition advance angle is a major task of adjusting the engine concerning emission standards, fuel consumption, torque value, etc. The results of the research showed that the process of optimizing the ignition advance curve can noticeably increase engine efficiency, as well as torque and power output from the engine while reducing fuel consumption as a result of lower indications of the air flow mass per second from MAF sensor (mass air flow sensor). The highest impact of the ignition advanced angle modifications can be seen in the area of the highest volumetric efficiency of the tested combustion engine. Almost no impact is observed within high engine speed levels. Simultaneously increasing engine load and rotation speed increases the possibility of engine knocking, which has a devastating effect on engine durability.

Key words: *combustion engine, ignition advance, ignition timing, efficiency, optimization*

1. Introduction

According to the latest emission standards and the power supply crisis in Europe, the efficiency of the combustion engine has increased in importance. Many vehicles in developing countries are aged. The average age of the vehicles in Poland is 14 years now. Furthermore, some of them are from the other continent, especially from North America where the exhaust emission standards differ from EU standards [3]. The growing interest in the USA import cars forces us to determine the optimum methods of readjustments and retrofitting engine control algorithms to adapt them to our environment. One of the critical parameters influencing engine efficiency is spark advance. As mentioned in articles [1, 8, 12, 13] depending on the quality of the factory ignition curve optimization process and basic emissions policies, past the process of the additional spark angle adjustments, gains in engine efficiency, can be as much as 20%. According to the study of Mobility and Vehicle Mechanics [4] if the flashpoint of fuel increases, requirements for the quality of the ignition also increase. An example of gas fuel with a higher than gasoline (480–530°C) flashpoint is CNG (545–800°C). Additionally CNG has a lower rate of flame speed propagation in relation to crank angle [10]. That phenomena induces necessity in recalibration factory settings of the powertrain control module to achieve correct efficiency. As Amr Ibrahim and Saiful Bair have shown [5] even exhaust gas recirculation strategy lowers the flame speed propagation which has to be compensated by adding spark advance, otherwise the engine will lose torque and fuel efficiency. CFD software simulations [6] confirm the increase in combustion pressure when approaching the optimum spark advance. As mentioned in [2, 7, 9, 11], increasing spark advance lowers the exhaust temperature due to a more complete burning process but simultaneously increases the NO_x emissions due to the ideal gas law which tells that an increase in pressure corresponds with a higher peak temperature.

2. Materials and methods

The experiment was performed using a car with an engine powered by gasoline and LPG fuel but for research purposes only gasoline fuel was used. A vehicle which has been chosen for the research is Ford Explorer 1996 4.0l V6 OHV, according to the high rate of popularity in Poland and officially selling the 1996 to 2001 models in Poland and Germany. Detailed vehicle specifications are presented in Table 1. Engine parameters are measured by the chassis dynamometer MAHA 4×4 (Table 2). Oil temperature is maintained around 100°C. Ambient and IAT temperature is held constantly during all tests. About the calculations of the PCM, except for dynamometer measurement of torque and power, graphs also contain the NET calculated value of torque and power by the Ford EEC V microchip. NET value is collected by the ForScan diagnosis software. The working bench diagram is shown in Fig. 1.

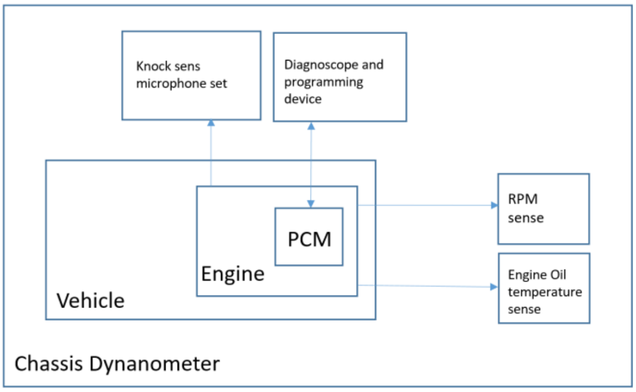

Fig. 1. Workbench diagram

Every dynamometer pull is repeated three times to calculate the correct average values. Knock detection is achieved by listening to the engine using an electronic stethoscope. Detailed names of tools used in research are detailed in Table 3. Spark advance is limited by the knock detection or the lower reading referring to the latest pull. Optimized spark advance values are uploaded to the PCM, past every change in the software, according to the KAM memory reset, the vehicle is idling for around 5 minutes.

Table 1. Vehicle and engine specification

Vehicle system	Detail
No. of cylinders	6-cylinder
Arrangement	V-type
Valve mechanism	12-valve OHV
Combustion chamber	Ford fast-burn
Manifolds	Parallel flow
Fuel System	Ford EFI SFI
Ignition system	Ford integrated EDIS
Control system	Ford EEC-V
Displacement	245 CID
Bore × Stroke	3.95×3.31 inches
Compression ratio	9.0:1
Power	119 kW@4200 rpm
Torque	323 Nm @2400 rpm
Firing order	1-4-2-5-3-6
Spark plug gap	0.054 inches (1.37 mm)
Base EEC catchword	LID0 → YZZ2
Transmission	Automatic 4R55E electronic control

PCM strategy is changed from LID0 to YZZ2 according to better data acquisition in YZZ2 versions and the origin of the software. LID0 is the first EU calibration for the 1996 model year while YZZ2 was used as a basic US model strategy for 1996 model year. The basic settings of PCM algorithms are the same. Differences in scalars are minor and do not have any influence on the car's performance. It refers especially to the differences in the mandatory existence of on-board emissions monitors (OBD1 EU vs OBD2 USA). Due to USA calibration data acquisition is easier on YZZ2 calibration than LID0.

Table 2. Chassis dynamometer

Name	Detail
Chassis dynamometer model	MAHA MSR 4×4 MSR 500/2
Measurement error	±2% of measured power

Table 3. Measurement, diagnosis and programming tools

Purpose	Detail
Diagnosis/programming	MongoosePro Ford
Programming software	Binary Editor 5.209
Diagnosis	ForScan 2.42
Diagnosis	Ford FJDS
Programming software	Binary Editor 5.209
Knock detection	Electronic Stethoscope
AFR measurement	STAG AFR
Oil temperature measurement	MAHA MSR 4×4 integrated sensor

To ensure that the environmental conditions are correct and constant, a heavy fan is installed in front of the experimental car. Final runs are performed on the same day with the same ambient temperature. Every run is conducted with the width open throttle (WOT), 3rd gear and locked lock-up clutch in a torque converter. Transmission and torque converter is switched to the manual operation by the CPU registers in the EEC V PCM.

The average Air to Fuel Ratio (AFR) is maintained around 0.84 lambda. It delivers the most boundaries of the knock occurrence. AFR changes in reach fuel areas have the minimal effect on the torque delivering of the engine so therefore no further changes in fuel Table are made. All boundary conditions are collected in Table 4.

Table 4. Environmental boundary conditions

Name	Value
Ambient temperature	15°C
Average AFR during pulls (WOT condition)	12.3 AFR
Fuel system status during pulls	OL
Gear	3. Manually locked by the CPU register
Lock up	Engaged. Manually locked by the CPU register
3rd gear ratio	1:1
Final gear ratio	3.73 Ford 8.8 LSD
IAT	20°C
Oil temperature during pulls	~100°C
Estimate rotating mass of the vehicle	100 kg
Rotating mass of the dynamometer	250 kg
Sum of the rotating mass	350 kg

All the values in Tables and graphs are presented in Newton-metre and horsepower due to the fact that the vast majority of calculations of the ECC V powertrain control module is also presented in this form. Output values from the PCM in PIDs do not present kilowatts. For easier and more accurate comparison between calculated values by the PCM and measured ones, horsepower was set as a main unit in the article.

3. Results

Figure 2 and Table 5 show the comparison of the results before and after the process of spark advance optimization. The most increase in the torque output can be observed in the low rpm areas. The biggest differences are presented at 2400 rpm for the power and at 2000 rpm for the value of torque. Most changes in the spark advance are achieved at 2400 rpm. After optimization, spark advance at 2400 rpm increased by 10.75 degrees to the total value of 21.5° referring to Table 6. Most significant points are bolded in red to emphasize the differences.

The highest absolute value of power is achieved at 3900–4000 rpm with the value of 93 horsepower (KM) which is equivalent to 69 (kW), while the peak of the torque occurs at 2800 rpm with the value of 190.84 Nm. Details for all rpm ranges are shown in Table 6.

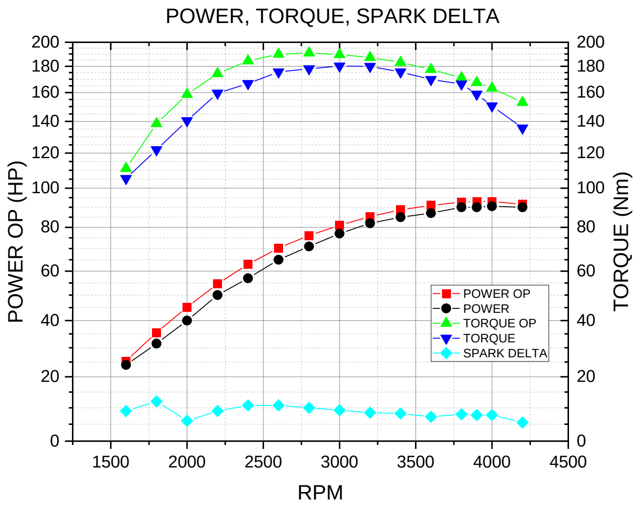

Fig. 2. Power, torque and spark delta before and after optimization

Table 5. Measurement data

n [rpm]	Power [HP] OP	Power [HP]	Delta [HP]	Torque [Nm] OP	Torque [Nm]	Delta [Nm]	SPARK° Delta
1600	25.3	24	1.3	111.03	105.32	5.71	9
1800	35.5	31.5	4	138.48	122.08	16.40	**12**
2000	45.2	40	5.2	158.69	140.43	**18.26**	6
2200	54.6	50	4.6	174.26	159.58	14.68	9
2400	63	57	**6**	184.32	166.67	17.65	**10.75**
2600	70.3	65	5.3	189.85	175.54	14.31	**10.75**
2800	76.1	71	5.1	**190.84**	178.04	12.80	10
3000	81	77	4	189.58	**180.22**	9.36	9.25
3200	85.3	82	3.3	187.17	179.93	7.24	8.50
3400	88.7	85	3.7	183.18	175.54	7.64	8.25
3600	91	87	4	177.49	169.69	7.80	7.25
3800	92.6	90	2.6	171.10	166.3	4.80	8
3900	**93**	90	3	167.44	158.86	8.58	7.75
4000	**93**	**90.5**	2.5	163.25	150.46	12.79	7.75
4200	91.5	90	1.5	152.97	135.64	17.33	5.50

Figure 3 shows the comparison between the calculated by the PCM NET torque and power values of the vehicle, before and after optimization. PCM calculated net values are represented by the estimated torque on the engine, minus implemented in the memory of the PCM, and Table of losses.

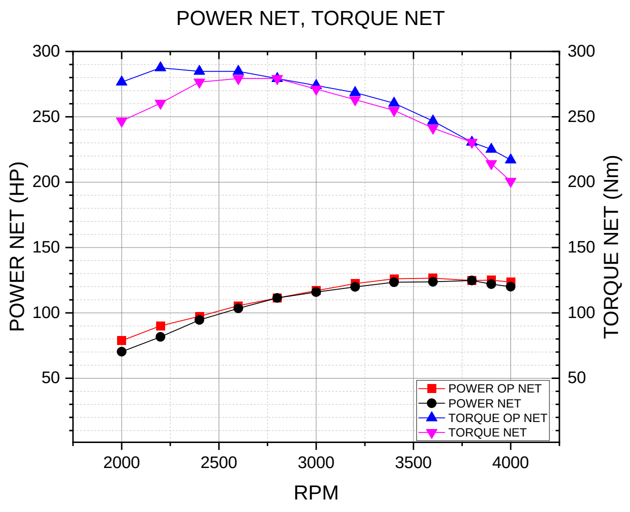

Fig. 3. Comparison between NET values before and after adjustments

Values of the NET torque should be higher than the dynamometer values according to the fact that the chassis dynamometer measures torque on the wheels, not directly engine torque. In the case of trying to measure the actual losses, by the chassis dynamometer, there is a demand to put the neutral gear, during the high wheel speed which can be dangerous for the automatic transmission, according to the lack of lubrication on the neutral gear. Specify values of the VE (Volumetric Efficiency) calculated by the PCM, air flow values (MAF) and the final spark advance, compared before and after the optimization, are shown in Table 6.

Referring to Table 6 and Figure 3 the highest value of the total spark advance is achieved at the highest rotation speed of the engine, independently of the process of optimization.

Table 6. Measurement data

n [rpm]	SPARK° OP	SPARK°	Delta [°]	VE(%) OP	VE(%)	Delta of VE	MAF[g/s] OP	MAF[g/s]	Delta of MAF [g/s]
2000	18.5	12.5	6	73.99	NaNd	NaNd	59.09	60.83	–1.74
2200	19.75	10.75	9	73.79	73.22	0.57	64.11	65.3	–1.19
2400	21	10.25	**10.75**	73.58	75.72	–2.14	70.12	70.82	–0.7
2600	21.5	10.75	**10.75**	73.9	76.05	–2.15	76.84	77.93	–1.09
2800	21.25	11.25	10	74.37	75.78	–1.41	83.56	84.4	–0.84
3000	21	11.75	9.25	74.92	75.28	–0.36	90.28	90.87	–0.59
3200	20.75	12.25	8.5	75.39	74.78	0.61	94.15	97.34	**–3.19**
3400	21	12.75	8.25	73.65	74.05	–0.4	98.27	100.07	–1.8
3600	21	13.75	7.25	71.44	71.9	–0.46	102.39	103.25	–0.86
3800	22.75	14.75	8	70.06	70.06	0	105.72	106.44	–0.72
4000	23.25	15.5	7.75	67.28	67.91	–0.63	104.39	107.01	–2.62
4200	23.75	17.25	6.5	59.99	63.91	**–3.92**	NaNd	107.21	NaNd
4400	24.75	19.25	5.5	NaNd	59.92	NaNd	NaNd	102.7	NaNd

Full graphs of the differences between spark advances angles are shown in Fig. 4.

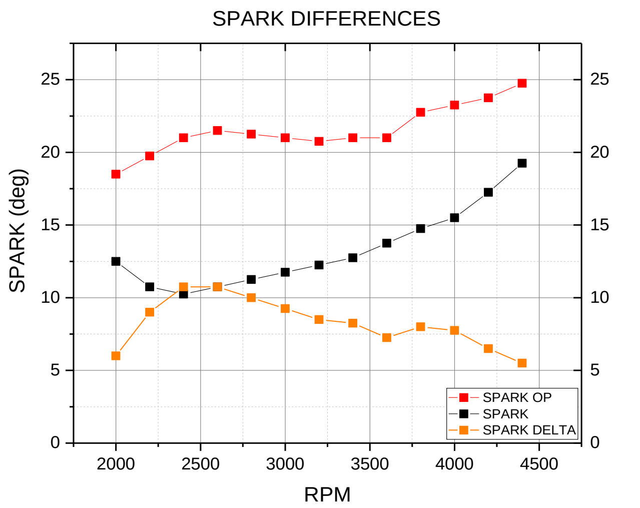

Fig. 4. WOT spark advance table values shared with a delta value

The final comparison between the PCM estimation and the chassis dynamometer values is presented in the shared Fig. 5. Values calculated by the PCM have shown a gain in torque output in the same manner as measured data by the dynamometer. However, values are different. Torque readings by the PCM cannot be used as a reference date in father research. Torque values shown by the PCM are correct only for indicating significant changes in power output.

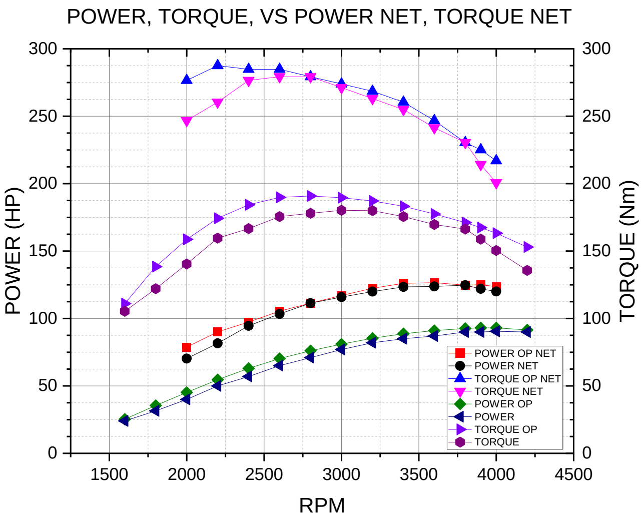

Fig. 5. Comparison between chassis dynamometer results and NET calculated values

There is a necessity of knowing that those values are based on mass air flow meter with conduct only changes in engine flows. Other physical phenomenon of the engine is not included in this type of calculation. As mentioned before NET values should be significantly higher according to the losses of the drivetrain.

4. Summary and conclusions

Optimization of the spark advance curve can significantly increase torque and power output from the engine, simultaneously reducing fuel consumption referring to the lowest indications of the air flow mass per second, from the MAF sensor. The highest gains can be observed in the area of the highest volumetric efficiency of the combustion engine which corresponds with the range of the highest torque output. Built-in functions of the Ford EEC V computer control unit give the possibilities for easy changes in main engine parameters like; fuel maps, spark advance maps, angles of injections maps etc. The flexibility of the PCM recalibration was proved by the results from the study. Changes in emissions from CARB to Europe OBD 2 (EURO 3 in this sample) were successfully achieved. No unintentional behavior of the engine was observed. No other parameters of the engine work significantly changed. The performance of the automatic transmission behavior was maintained. Highest improvements were achieved at the rate of 11.5% in power @2400 rpm and 13% in torque @2000 rpm. The most significant efficiency gain was observed at 3200 rpm with a value of 3.3%. The greatest spark advance change occurred at 2400 and 2600 rpm amounted to 10.75°.

Nomenclature

AFR	air fuel ratio
CFD	computational fluid dynamics
CNG	compressed natural gas
ECU	electronic control unit
EDIS	electronic distributor less ignition system
EEC	electronic engine control
EFI	electronic fuel injection
IAT	input air temperature
KAM	keep alive memory
LPG	liquefied petroleum gas
MAF	mass air flow
OHV	overhead valves
OL	open loop
PCM	powertrain control module
VE	volumetric efficiency
WOT	wide open throttle

Bibliography

[1] Ehsan M. Effect of spark advance on a gas run automotive spark ignition engine. J Chem Eng. 2010;1:42-49. https://doi.org/10.3329/jce.v24i0.5584

[2] El-Sharkawy MR, Abaskharon MBR, Abd-El-Tawwab AM, Ezzat Fawzy MH. Effect of static spark timing on the performance and emissions of a spark ignition engine using CNG. IOP Conf Ser Mater Sci Eng. 2019;518(3):12. https://doi.org/10.1088/1757-899X/518/3/032062

[3] General D. Internal FOR. Comparative study on the differences between the EU and US legislation on emissions in the automotive sector. Inst Eur Environ Policy. 2015;53(9): 1689-1699. https://doi.org/10.2861/503165

[4] Hristov R, Bogdanov K, Dimitrov R. Research the influence of spark plugs types on the performance of the engine operating on gaseous fuels. Mobility & Vehicle Mechanics. 2018;44(1):51-61. https://doi.org/10.24874/mvm.2018.44.01.05

[5] Ibrahim A, Bari S. A comparison between EGR and lean-burn strategies employed in a natural gas SI engine using a two-zone combustion model. Energy Convers Manage. 2009;50(12):3129-3139. https://doi.org/10.1016/j.enconman.2009.08.012

[6] Joshi A, Borse S. Study of the effect of spark advance, engine speed variation and number of spark plugs on engine performance using CFD software. Journal of Ocean, Mechanical and Aerospace. 2017;48(48):1-9. https://doi.org/10.36842/jomase.v48i1.170

[7] Lungu J, Siwale L, Luwaya E. Study and effect of ignition timing on the combustion characteristics of gasoline En 91 in a spark ignition engine. NAER-V1. 2021;104-2. https://doi.org/10.9734/bpi/naer/v1/7257D

[8] Marzec P. Tests of a SI engine powered by gaseous fuels blends of LPG + DME of various proportions with variable load. Combustion Engines. 2022;190(3):23-26. https://doi.org/10.19206/CE-144124

[9] Nawazish Mehdi S, Yousufuddin S. Effect of ignition timing, equivalence ratio, and compression ratio on the performance and emission characteristics of a variable compression ratio SI engine using ethanol-unleaded gasoline blends. International Journal of Engineering. 2008;21(1):97-106. https://www.ije.ir/article_71695_6566994fbcdb15e1ad6711b147c8c9a5.pdf

[10] Ramasamy D, Kadirgama K, Rahman M, Zainal Z. Analysis of compressed natural gas burn rate and flame propagation

on a sub-compact vehicle engine. International Journal of Automotive and Mechanical Engineering. 2015;11(1):2405-2416. https://doi.org/10.15282/ijame.11.2015.21.0202

[11] Tribbett EJ, Froehlich EM, Bayer L. Effects of ignition timing, equivalence ratio and compression ratio on RDH engine performance. 2002. https://api.semanticscholar.org/CorpusID:17643397

[12] Tunka L, Polcar A. Effect of various ignition timings on combustion process and performance of gasoline engine. Acta Univ Agric Silvic Mendelianae Brun. 2017;65(2):545-554. https://doi.org/10.11118/actaun201765020545

[13] Zareei J, Kakaee AH. Study and the effects of ignition timing on gasoline engine performance and emissions. Eur Transp Res Rev. 2013;5(2):109-116. https://doi.org/10.1007/s12544-013-0099-8

Adam Kamiński, MSc. – Faculty of Mechanical Engineering, Wroclaw University of Science and Technology, Poland.

e-mail: *adam.kaminski@pwr.edu.pl*

Maria Skrętowicz, DEng. – Faculty of Mechanical Engineering, Wroclaw University of Science and Technology, Poland.

e-mail: *maria.skretowicz@pwr.edu.pl*

Konrad Krakowian, DEng. – Faculty of Mechanical Engineering, Wroclaw University of Science and Technology, Poland.

e-mail: *konrad.krakowian@pwr.edu.pl*

Mateusz Kupski, Eng. – Faculty of Mechanical Engineering, Wroclaw University of Science and Technology, Poland.

e-mail: *mateusz.kupski@pwr.edu.pl*